Article

Design and Experimental Study of a Cleaning Device for Edible Sunflower Harvesting

Xingyu Yang [1,2], Xiaoxiao Sun [1,2], Bin Li [1,2,*], Yang Liu [1], Shiguo Wang [1], Xiaolong Gao [1,2] and Yuncheng Dong [1]

[1] Institute of Mechanical Equipment, Xinjiang Academy of Agricultural and Reclamation Science, Shihezi 832000, China; yangxingyu@stu.shzu.edu.cn (X.Y.); sunxiaoxiao@stu.shzu.edu.cn (X.S.); maoyinghui0701@shzu.edu.cn (Y.L.); 20192309011@stu.shzu.edu.cn (S.W.); gaoxiaolong@stu.shzu.edu.cn (X.G.); dongych2024@163.com (Y.D.)

[2] School of Mechanical and Electrical Engineering, Shihezi University, Shihezi 832000, China

* Correspondence: bin175337620@shzu.edu.cn

Abstract: Existing cleaning devices for edible sunflower have a low cleaning efficiency, high cleaning loss rate, and high impurity rate; therefore, a wind-sieve-type cleaning device for edible sunflower harvesting was designed. According to the characteristics of dislodged objects, a vibrating screen for the device was designed, and the dislodged edible sunflower objects in the device were used for a mechanical analysis of the force conditions to determine the displacement of the different edible sunflower objects dislodged by the action of airflow. Using FLUENT-DEM gas–solid coupling simulation technology, the velocity of the flow field, the velocity vector, and the trajectory of the dislodged objects inside the cleaning device were analyzed, and the law of motion applied to the airflow and the dislodged objects inside the device was clarified. According to the results of the coupled simulation analysis, the key factors affecting the operation of the cleaning device were wind speed, vibration frequency, and amplitude. Based on the key factors of wind speed, vibration frequency, and amplitude, an orthogonal rotary combination test was carried out with the loss rate and impurity rate of cleaned grains as the evaluation indexes, and the test parameters were optimized to obtain the optimal combination of operating parameters of the device, which were as follows: wind speed: 30 m·s^{-1}; vibration frequency: 8.44 Hz; and amplitude: 41.35 mm. With this combination of parameters, the seed loss rate and impurity rate reached 3.47% and 6.17%, respectively. Based on the optimal combination of operating parameters, a validation test was performed, and the results of this test were compared with the results of the test bench using this combination of parameters. The results show that the relative errors of the loss rate and impurity rate between the bench test and the simulation test were 3.45% and 3.07%, respectively, which are less than 5%, proving the reliability of the simulation analysis and the reasonableness of the design of the test bench.

Keywords: edible sunflower; cleaning device; FLUENT-DEM gas–solid coupling; simulation analysis

1. Introduction

Edible sunflowers are cash crops that are widely grown and consumed in China due to their ability to adapt to harsh growing environments, their short harvesting cycle, and their significant economic benefits [1]. Chinese people highly favor sunflower seeds due to their pleasant taste. In recent years, China's sunflower seed export value has been increasing annually. In 2020, China's sunflower seed exports reached USD 648 million, a year-by-year increase of 4.35%. By 2022, China's sunflower seed consumption is expected to reach 2.5 million tons, with total sales reaching CNY 78 billion [2]. China's sunflower industry is among the world's leading industries, and the world sunflower industry center is accelerating its transfer to China [3]. A reliable and efficient sunflower cleaning device is one of the key factors that ensure the rapid development of the sunflower industry. However, the cleaning technology for sunflowers is still in the early stages of development. Sunflower

cleaning devices mainly rely on modifications of other crop harvesters or imitations of imported foreign technology, with most of them designed to ensure low loss rates, often at the expense of cleaning efficiency [4,5]. In comparison to other crops, sunflower cleaning technology is notably outdated [6–9].

The quality of the final edible sunflower seed harvest is directly determined by the performance of the cleaning operation, which is an important process in mechanical harvesting. Domestic and foreign research has achieved results using a scavenging device. Kiurchev et al. [10] investigated the effectiveness of an air suction scavenging device in separating seeds from dislodged objects and achieved high efficiency in seed separation through airflow velocity. Yuko conducted a simulation of the scavenging process using FLUENT technology to analyze the airflow distribution within a scavenging device. The results revealed the distinctive law of distribution of the airflow in the device and clarified the significant characteristics of the wind force inside the device [11]. A study conducted by Priporov et al. also summarized and clarified the significant characteristics of the wind force inside the device [11]. The seed cleaning process was analyzed mathematically, and a corresponding model was established. Based on this analysis, the grain cleaning device was improved to adapt to sunflower cleaning [12,13]. G. Craessaerts investigated the movement of objects under the interaction of a fan and vibrating sieve, as well as the loss of objects [14–16]. E. Sultanovitch investigated the changes in mass and volume of an object during its movement in a scavenging device and summarized the corresponding calculation formula [17]. Jfattahi et al. [18] designed a high-pressure roller sunflower-seed-sorting machine based on the characteristics of sunflower dislodgement with a certain amount of electric charge. Zhang J.X. developed a vertical oil sunflower threshing and cleaning device based on the centrifugal principle, which removed dislodged objects from the sunflower using the airflow of the fan and the rotation of the wind separator cylinder [19]. Pan Z.Y. used Matlab2010 (Matlab2010 is a commercial math software developed by Mathworks, Inc. in the United States.) to establish a mathematical model of the distance between the fan deflector and the blades, and optimized the calculation of the parameters of the device, which improved the performance of the device cleaning [20]. Liu K. used the gas–solid coupling method to deeply analyze the cleaning process of rice grains in the device, clarified the distribution of the pressure formed by the airflow in the device, and obtained the law of the influence of wind on the state change in the grains [21]. Combined with the above research, it can be seen that the existing research provides a theoretical basis and research methods to conduct research on a sunflower scavenging device to a certain extent, but there has been less research on scavenging devices for sunflowers, and there has been no full consideration of the characteristics of sunflowers, so the adaptability of the device is low, it cannot effectively scavenge different varieties of sunflowers under different growing conditions, and it has difficulty effectively dealing with the separation of sunflower stalks and grains. Because of the difficulty in effectively dealing with the separation of straw and seeds of sunflower, after cleaning, the seeds are mixed with more straw and impurities, resulting in a low cleaning efficiency.

This paper presents the design of a wind-sieve-type cleaning device for edible sunflower harvesters, addressing the issues of low cleaning efficiency, a high cleaning loss rate, and a high impurity rate. The device was designed based on the characteristics of edible sunflower. The distribution of airflow in the cleaning device and the movement trajectory of sunflower particles were analyzed to determine the key factors affecting the device's effectiveness. The device's cleaning effectiveness was analyzed using an orthogonal simulation test under various conditions to determine the optimal working parameters. The results of the bench test and simulation test were compared and analyzed using the optimal parameters through a validation test to confirm the reliability of the simulation test and the reasonableness of the test bench design. The device has improved the current situation in Xinjiang, where there is a lack of cleaning devices specifically designed according to the characteristics of edible sunflower seeds, thus enhancing the cleaning efficiency of the

edible sunflower. This provides a reference for the design and improvement of future sunflower cleaning devices.

2. Materials and Methods

2.1. Overall Structure of the Cleaning Device

The structure of the cleaning device is shown in Figure 1. At the top of the device is the vibrating plate, which receives the edible sunflower discharged material; the middle of the device is the upper sieve, which is responsible for the initial screening of the discharged material. The lower part of the device consists of the lower sieve and the cross-flow fan, the sunflower discharged material in the lower sieve to be cleaned for the second time, and the cross-flow fan can produce a certain speed of airflow with the upper sieve and the lower sieve for the discharged material to be cleaned. The single-arm rocker and double-arm rocker drive the upper and lower sieves by cooperating with each other.
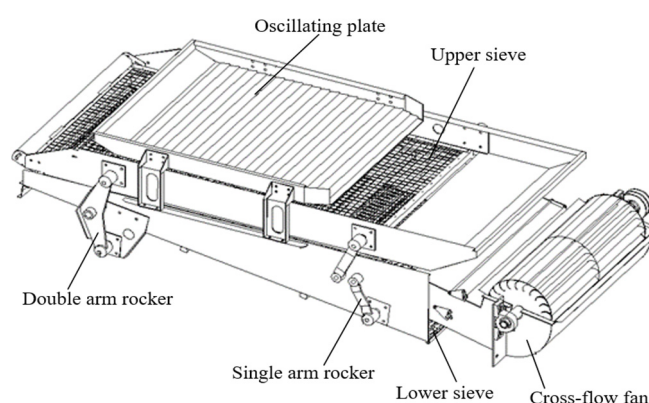
Figure 1. Structure of cleaning device.

2.2. Working Principle of the Cleaning Device

When the cleaning device is in operation, the single and double arm rockers move in unison, propelling the upper and lower sieve plates to move back and forth in opposite directions, while the blades of the cross-flow fan begin to rotate, creating a stable and evenly distributed airflow. After the threshing process, the edible sunflower extracts fall onto the vibrating plate, and since the vibrating plate shakes regularly under the drive of the upper sieve, the edible sunflower extracts falls onto the upper sieve in a regular manner. With the collaboration of the upper sieve and the airflow of the fan, the impurities such as stalks are blown out of the working area, while the large impurities isolated by the upper sieve plate are discharged from the surface of the sieve plate with the nonstop reciprocating motion of the upper sieve plate. The seeds and smaller impurities that have successfully passed through the upper sieve plate will fall to the lower sieve plate, which has smaller holes that the sunflower seeds cannot pass through. Some of the smaller impurities will pass through the lower sieve plate with the constant movement of the lower sieve plate, and the other part will be carried away by the airflow. As the lower sieve is inclined, the seeds separated on the lower sieve will pile up on the inclined side under the action of the lower sieve and finally slide down to the receiving opening to complete the cleaning of the seeds.

2.3. Design of Vibrating Sieve

2.3.1. Overall Design of Vibrating Sieve

The vibrating sieve plays a vital role in the wind-sieve-type cleaning device. The efficiency of the cleaning device is contingent upon the design of the vibrating screen, which directly affects the device's operational performance. Generally, the ratio of the length-to-width of the vibrating sieve is 2–3 [22]; therefore, the device has an aspect ratio of 2.21, which meets the requirements. To accommodate the dimensions of the threshing

device and facilitate installation, the parameters of the vibrating sieve plate are designed as shown in Table 1.

Table 1. Structural parameters of the vibration sieve.

Name	Value
Length × width (upper sieve)	1991 mm × 900 mm
Length × width (lower sieve)	458 mm × 900 mm
Length × width (Tailing sieve)	1784 mm × 900 mm
Lower sieve installation angle	8°
Relative distance between upper and lower sieve	104 mm
Woven sieve with square hole (upper sieve)	20 mm × 20 mm
Radius of round hole sieve (lower sieve)	4 mm
Size of long hole sieve (lower sieve)	10 mm × 4 mm

2.3.2. Vibrating Sieve Hole Design

A vibrating sieve is a type of equipment used for sorting materials. It is usually divided into an upper sieve and a lower sieve, each responsible for a distinct screening task. The upper sieve is used for coarse screening, aimed at preventing larger impurities, such as sunflower disk and stalks, from entering the lower sieve. On the other hand, the lower sieve is used for fine screening, with the primary function of separating sunflower seeds.

Woven sieves are usually square hole sieves, which are widely used due to their simple structure and sufficient effective screening area. This type of sieve is conducive to the passage of materials, but there are shortcomings in its screening performance, especially in the sieve hole size. Larger holes may allow small impurities to pass through, while smaller holes may be clogged due to the material and affect the screening effect. Therefore, woven sieves with square holes are suitable for initial screening. The perforated screen's strong screening performance is due to the adjustable shape of its holes, which can be round or long. Accordingly, in consideration of the distinctive attributes of each sieve type and the relative merits of screening efficiency and accuracy, the woven sieve with square hole is selected as the upper sieve, facilitating the passage of materials and coarse screening. The lower sieve is designed as a combination of "round hole sieve + long hole sieve", which guarantees the screening effect and, at the same time, ensures that seeds falling horizontally as well as vertically can pass through the sieve mesh, in order to minimize the loss of seeds, thus obtaining the most optimal cleaning effect. The three forms of sieves are shown in Figure 2.

(a)   (b)   (c)
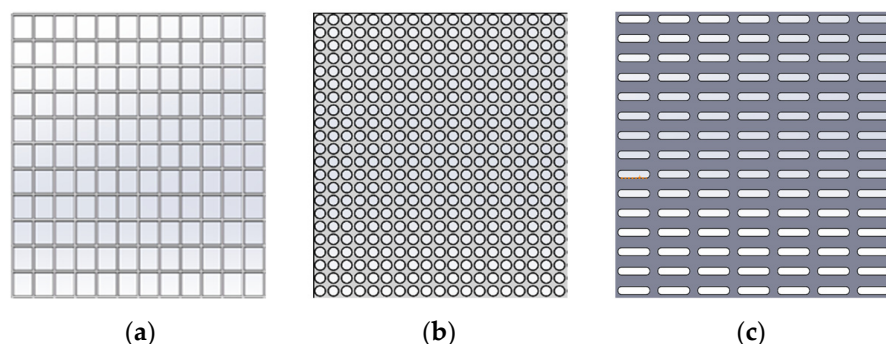
Figure 2. Structure of vibrating sieve. (**a**) Square hole sieve. (**b**) Round hole sieve. (**c**) Long hole sieve.

2.4. Motion Analysis of Vibrating Sieve

The relative motion of edible sunflower dislodged material on the surface of the vibrating screen is primarily influenced by two key factors: the acceleration of the vibrating sieve and the angle between the dislodged material and the sieve surface. To analyze the motion characteristics of the edible sunflower dislodged material, we employ kinematic–static analysis, which enables the examination of the motion of the dislodged material. For

the sake of analysis, we assume that the rockers driving the vibrating screen exhibit no length difference, that they are parallel to each other, and that the radius of rotation of the crankshaft is negligible. These assumptions allow the motion of the mechanism to be regarded as linear. The movement of the vibrating screen is illustrated in Figure 3.
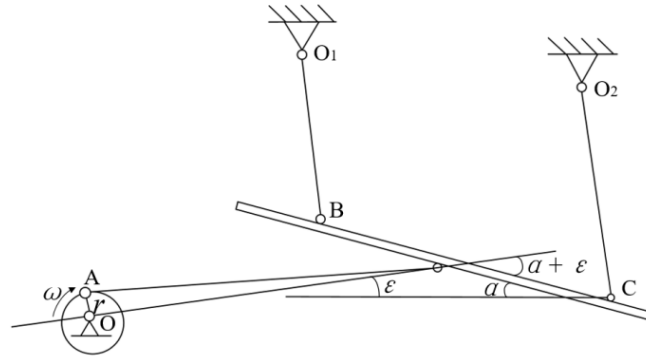
Figure 3. Movement of vibrating screen, where ω is angular speed of crankshaft rotation, rad·s^{-1}; r is radius of rotation of crank, m; α is the angle of the lower sieve swinging, °; $\alpha + \varepsilon$ is the angle between the direction of the lower sieve swinging and the sieve surface, °.

The motion of edible sunflower dislodged material from the vibrating screen must satisfy the following conditions:

$$\begin{cases} \frac{g \cdot \sin(\alpha+\varphi)}{\cos(\varepsilon+\alpha+\varphi)} = K\text{x} \\ \frac{g \cdot \sin(\varphi-\alpha)}{\cos(\varepsilon+\alpha-\varphi)} = K_{\text{y}} \\ \frac{g \cdot \cos \alpha}{\sin(\varepsilon+\alpha)} = K_{\text{p}} \end{cases} \tag{1}$$

In Equation (1), Kx is the acceleration of the material in the horizontal direction, m·s^{-2}; K_{y} is the acceleration of the material in the vertical direction, m·s^{-2}; K_{p} is the acceleration of the material when it is thrown up, m·s^{-2}.

To ensure that the cleaning device can effectively stratify different edible sunflower dislodged materials, it is essential to allow them to perform parabolic motion on the vibrating sieve. Additionally, to guarantee continuous sieving of the edible sunflower dislodged material on the sieve surface, it is necessary that the horizontal displacement of the parabolic motion be at least equal to the vertical displacement. Therefore the magnitude relationship between K_{s}, K_{x}, and K_{p} has to be satisfied: $K_{\text{p}} < \omega^2 r > K_{\text{y}} > K_{\text{x}}$ [23].

In addition, the appropriate settings of the upper and lower sieve swing and inclination are crucial for achieving efficient screening. To ensure uniform distribution of the material on the screen surface and to guarantee both screening accuracy and efficiency, it is necessary to control the swing of the upper and the lower sieves within the range of 35 to 45 mm, while maintaining an inclination of the upper sieve. The angle between lower sieve swing direction and the sieve surface should be set to 4°. Furthermore, the upper sieve inclination angle and the lower sieve inclination angle should be set to 0° and 8°, respectively.

2.5. Force Analysis of the Edible Sunflower Dislodged Material

In order to predict the movement distance of each dislodged object on the surface of the device, it is necessary to analyze the stress condition of the dislodged object when it is thrown up. This is shown in Figure 4, which depicts the force analysis diagram.
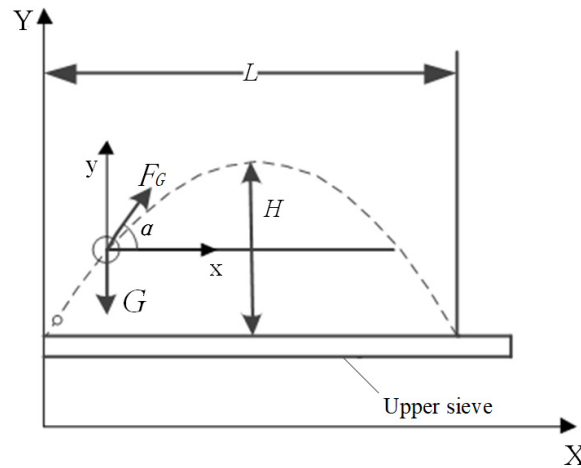
Figure 4. The state of force when the material is thrown up, where G is gravity, N; F_G is the wind force on the object, N; α is the gas blow-in angle, °; L is the horizontal displacement of the dislodged object, m; H is the vertical displacement of the dislodged object, m.

The specific analytical formula is shown in Equation (2).

$$
\begin{cases}
G = mg \\
G - F_G \sin \alpha = m a_y \\
F_G \cos \alpha = m a_x \\
F_G \sin \alpha > G \\
F_G = k\rho S v^2
\end{cases}
\tag{2}
$$

In Equation (2), m is the mass of the dislodged object, kg; a_y is the vertical acceleration, m·s^{-2}; a_x is the horizontal acceleration, m·s^{-2}; k is the coefficient of resistance of an object transporting work in air; ρ is the density of air, kg·m^{-3}; and v is the speed of wind, m·s^{-1}; S is the projected area of the object on the normal airflow plane, mm^2.

The capacity of an object to attain stationary levitation in the presence of vertical airflow is contingent upon the equilibrium between the forces exerted by the airflow and the gravitational force. This equilibrium is reached when the velocity of the airflow reaches a specific critical velocity, v_t. At this point, the thrust of the rising airflow on the object is precisely balanced by the downward force on the object due to gravity. Should the airflow velocity increase beyond the critical velocity, the momentum of the airflow will exceed the gravitational force of the object, resulting in an upward movement. Conversely, when the airflow velocity is insufficient to support the object, it will fall due to gravity. The critical velocity can be calculated using Equation (3).

$$
v_t = \left(\frac{mg}{\rho k S} \right)^{\frac{1}{2}}
\tag{3}
$$

The trajectory of the vibrating sieve in space is driven by the crank linkage and tends to be sinusoidal during the cleaning operation. The time spent in one motion cycle of the edible sunflower dislodged material is designated as t. The horizontal displacement L and vertical displacement H of the edible sunflower dislodged material are illustrated in Equation (4).

$$
\begin{cases}
H = A \sin \omega t \\
L = \dfrac{v_0^2 \sin \theta \cos \theta}{a_y} + \dfrac{a_x (v_0 \sin \theta)^2}{2 a_y^2}
\end{cases}
\tag{4}
$$

In Equation (4), A is the amplitude, mm; ω is the angular velocity of the device, rad·s^{-1}; v_0 is the initial velocity of the material being thrown, m/s; θ is the angle between the initial velocity of the material and the horizontal plane, °.

Equation (5) can be obtained by combining Equations (3) and (4):

$$\begin{cases} L = \frac{v_0^2 m \sin\theta \cos\theta}{mg - k\rho Sv^2} + \frac{k\rho Sv^2 m^2 \cos\theta (v_0 \sin\theta)^2}{2(mg - k\rho Sv^2)^2} \\ H = A\sin\omega \frac{mv_0}{mg - k\rho Sv^2} \end{cases} \tag{5}$$

The analysis of Formula (5) reveals that on the vibrating screen, the displacement in the horizontal direction and the displacement in the vertical direction of the three types of the edible sunflower dislodged material are as follows: edible sunflower petiole, edible sunflower plate (broken), and edible sunflower seed, in descending order of magnitude.

2.6. FLUENT-DEM Coupled Simulation Analysis

To clarify the size of the airflow velocity in different regions of the cleaning device and the change in airflow direction in each region, as well as to analyze the change rule of the movement of the dislodged material of sunflower when subjected to the external force generated by the device, we simulated the cleaning process of sunflower seeds based on the FLUENT-DEM gas–solid coupling technology. Using FLUENT18.0 (This software is produced by ANSYS, a company located in Pittsburgh, USA.) to design the parameters of the airflow field, the distribution of the airflow field inside the device was simulated and calculated, and the calculation results were transferred to EDEM. Subsequently, particle models of edible sunflower plates (broken), edible sunflower petioles, and edible sunflower seeds were created in EDEM2018 (EDEM2018 is a discrete meta-analysis software produced by DEM Solutions (DEMSL), a UK-based company.), which could simulate the stress situation, velocity change, and displacement of the corresponding materials under the action of the airflow.

2.6.1. Grid Division of the Device

Before the meshing process, it is necessary to simplify the device model to avoid an increase in the computational burden of the software, which would result from the large number of sieve holes present in the scavenging device [24]. The simplified model is then meshed using Workbench, with the surface mesh size controlled as follows: minimum size 4 mm, maximum size 45 mm, growth rate 1.2, size function using curvature proximity analysis method, curvature normal angle of 10°, and the gap-filling unit layer number is 5 layers. The face mesh repair tool is used to merge free nodes and eliminate free faces, improving face mesh quality. Through Diagnosis diagnostic tool detection, the maximum distortion rate (maximum "skewness") is 0.537, indicating that the quality of face meshing is high. The effect of this process is illustrated in Figure 5.
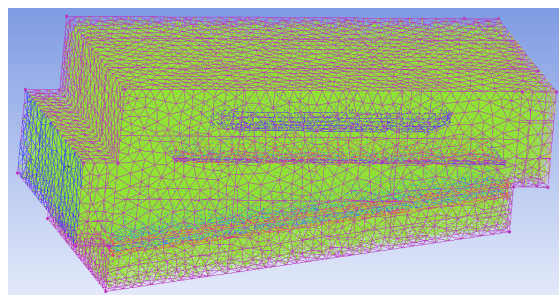
Figure 5. Mesh model of cleaning device.

2.6.2. Airflow Velocity Distribution in the Device

The device's airflow produces dynamic alterations, resulting in the formation of airflow fields with unique properties. These various airflow fields exert different forces and have distinct effects on the edible sunflower dislodged material. For the same air pressure difference, the smaller the hole through which the airflow passes, the greater its velocity. Consequently, the FLUENT18.0 (This software is produced by ANSYS, a company located

in Pittsburgh, USA.) was employed to simulate the airflow field of the device with the objective of elucidating the characteristics of the airflow field in distinct areas of the device. The simulation results are presented in Figure 6.
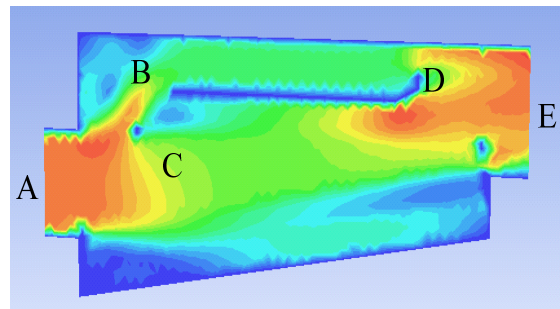
Figure 6. Cloud diagram of velocity distribution in cleaning device. (**A**) Air inlet. (**B**) Upper air inlet. (**C**) Lower air inlet. (**D**) Shaking plate. (**E**) Air outlet.

The airflow entering through the inlet A is divided into two channels, the upper inlet B and the lower inlet C, by the action of the dither plate D. The airflow creates a region of low wind speed above the dither plate D, effectively reducing the impact force on the edible sunflower dislodged material. The dislodged materials initially fall onto the upper sieve, where they are initially separated under the influence of the backward airflow generated by the lower inlet C. The light sunflower plate fragments and petioles are eliminated from the cleaning system by the airflow, while the remaining objects enter the lower sieve under the effect of vibration and gravity. In this process, the synergistic effect between the airflow generated by the lower inlet C and the vibrating screen enables the secondary cleaning of the sunflower seeds. This process is highly effective in removing impurities and ensures that the sunflower kernels are collected effectively in the receiving box. Furthermore, the low air velocity zone formed below the air inlet A significantly reduces the loss of seeds due to airflow during the collection process. Concurrently, the higher air velocity zone formed at the air outlet E enhances the separation efficiency of the light mass impurities, significantly reducing the impurity content of the cleaning device.

2.6.3. Analysis of Velocity Vectors in the Device

The investigation of the distribution of internal velocity vectors is of particular importance when studying the performance of the scavenging device. By analyzing the change in velocity vector within the device, the change in the motion of the edible sunflower dislodged material under the influence of different airflow velocities can be obtained. The result of velocity vector distribution is demonstrated in Figure 7. In the figure, wind velocity at the dark blue line > wind velocity at the sky blue line > wind velocity at the green line > wind velocity at the yellow line.
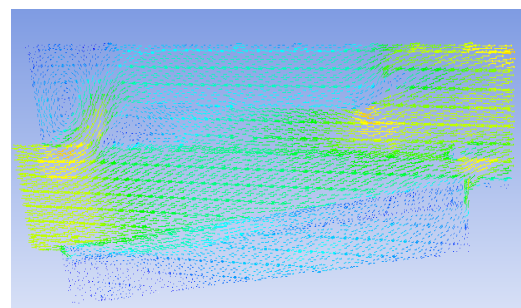
Figure 7. Cloud diagram of velocity vector distribution in cleaning device.

As can be seen from Figure 6, when the airflow enters the cleaning device from the air inlet, it is divided into two airflows upward and downward due to the presence of the

shaking plate. Since the airflow near the shaking plate has a lower velocity, the movement path of the material is affected. In addition, when the upward airflow in the device meets the downward airflow near the shaking plate in space, the two airflows mix together to form a vortex, which helps to accelerate the falling of the material when the vortex is formed at a position below the shaking plate. When the airflow passes through the air outlet, the airflow speed rises because the volume of the space in which the airflow is located decreases, thus facilitating the rapid cleaning of impurities and further improving the overall cleaning efficiency of the device.

2.7. Motion Simulation Analysis

2.7.1. Particle Modeling of the Edible Sunflower Dislodged Material

The accurate modeling of material particles is of paramount importance in the simulation of cleaning devices [25]. The real-size modeling of the edible sunflower dislodged material was performed using SolidWorks2018 (SolidWorks2018 is a 3D modeling software produced by a subsidiary of Dassault Systemes, which is located in Massachusetts, USA.). And the model was converted to IGES format for simulation analysis in EDEM2018. Leveraging the findings of the team's investigation into the parameters pertinent to the discrete element simulation of edible sunflower Sanrui 39 in the preliminary stage [26], the discrete element parameters of edible sunflower particle model were designed in EDEM (Tables 2 and 3). Subsequently, these particles were filled in the material model, and the filled material model is shown in Figure 8.

Table 2. Mechanical characteristic parameters of the edible sunflower dislodged material.

Name	Modulus of Elasticity/MPa	Modulus of Shearing/MPa	Poisson Ratio	Density/kg·m^{-3}
Edible sunflower seed	147.6	56.3	0.31	346
Edible sunflower disk	92.4	35.5	0.30	679
Edible sunflower petiole	33.4	53.1	0.26	331

Table 3. Contact parameters of the edible sunflower dislodged material.

Material	Static Friction Coefficient	Collision Recovery Coefficient	Coefficient of Rolling Friction
Edible sunflower seed with edible sunflower seed	0.57	0.57	0.01
Edible sunflower seed with edible sunflower disk	0.55	0.67	0.01
Edible sunflower seed with edible sunflower petiole	0.54	0.53	0.01
Edible sunflower disk with edible sunflower disk	0.81	0.56	0.01
Edible sunflower disk with edible sunflower petiole	0.82	0.40	0.01
Edible sunflower petiole with edible sunflower petiole	0.83	0.48	0.01
Edible sunflower seed with rigid sieve disk	0.73	0.58	0.01
Edible sunflower disk with rigid sieve disk	0.61	0.50	0.01
Edible sunflower petiole with rigid sieve disk	0.78	0.50	0.01

(a)   (b)   (c)
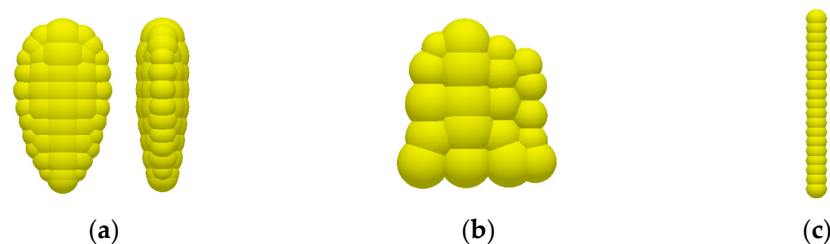
Figure 8. Particle model of the edible sunflower dislodged material. (**a**) Sunflower seed. (**b**) Sunflower disk (broken). (**c**) Sunflower petiole.

2.7.2. Analysis of the Law of Motion of the Edible Sunflower Dislodged Material

The working performance of the cleaning device can be effectively improved by analyzing the movement law of the dislodged material of the edible sunflower on the vibrating sieve and its interaction with other material [27].

After processing the simulation results of airflow field simulation by EDEM2018, various types of the edible sunflower dislodged materials were generated within the device and the dislodged materials were allowed to move in the device; the simulation results obtained are shown in Figure 9, Figure 10, and Figure 11, respectively.
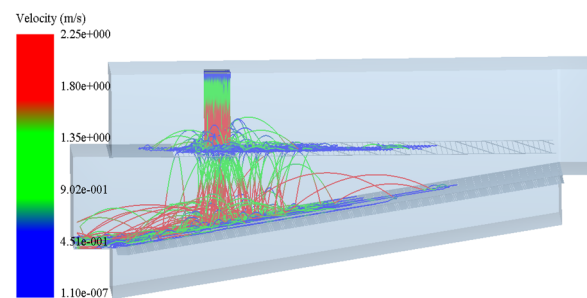
Figure 9. Motion track of sunflower seeds.
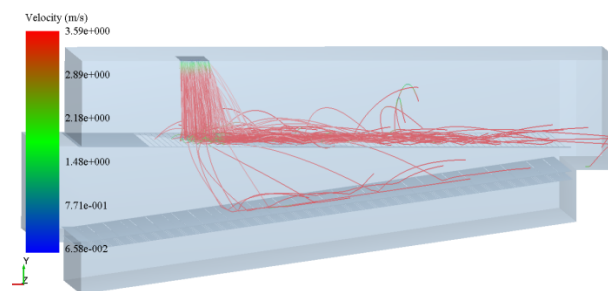
Figure 10. Motion track of sunflower disk (broken).
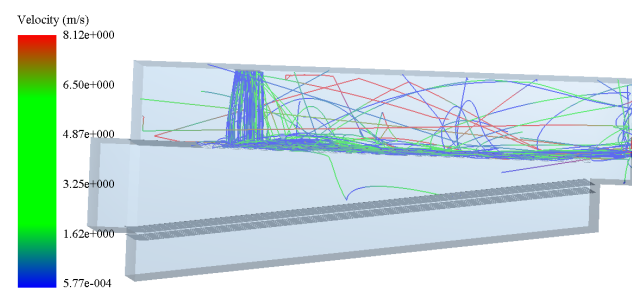
Figure 11. Motion trajectory of sunflower petiole.

The trajectory of the edible sunflower seeds is shown in Figure 9. It shows that when the seeds enter the upper sieve of the cleaning equipment, they begin to move significantly toward the rear end of the equipment under the combined action of the airflow generated by the fan and the vibration of the equipment. After the seeds enter the lower sieve, they continue to make a parabolic movement and gradually approach the receiving box. Due to the continuous contact with the vibrating sieve surface, the kinetic energy of the seeds is gradually reduced, causing the height of their parabolic movement on the sieve surface to gradually decrease. The decreasing kinetic energy not only affects the trajectory of the seeds, but also has an effect on the screening efficiency. Because of the small size of the edible sunflower seeds, they can pass through the screen holes earlier to realize the effective separation from the larger materials. As can be seen from the figure, the speed of airflow shows a tendency of gradual decrease, the closer to the end, the smaller the airflow speed;

therefore, the cleaning of the edible sunflower dislodged material by wind force occurs mainly in the front and middle regions of the vibrating sieve.

The trajectory of the sunflower disk (broken) is shown in Figure 10. It can be observed that the movement of the sunflower disk (the larger part) is mainly carried out in the upper sieve, and some disks will fall through the woven sieve holes into the lower sieve. This phenomenon is primarily attributed to the size of the airflow resistance of the sunflower disk, which is related to its area and significantly larger than that of the stem and the sunflower seeds. At the front end of the vibrating sieve, due to the high number of contacts between the disk, the seeds, and the stem, the loss of sunflower disk kinetic energy at the time of contact is more significant. And, as the sunflower seeds fall through the upper sieve to the lower sieve, the number of mutual collisions between the material is reduced. The sunflower disk in the middle of the device kinetic energy loss is less than its loss of kinetic energy in the front; as a result, the height of the sunflower disk at the middle end of the vibrating screen is higher than the front.

The trajectory of the edible sunflower petiole is shown in Figure 11. As can be seen from Figure 11, due to its larger size and lower density, the petiole experiences more pronounced displacement change in all directions under the action of the same intensity of wind force. The petiole will be separated from other dislodged materials first when subjected to the wind force exerted by the airflow and the upward force exerted by the vibrating sieve, so the petiole avoids a large number of collisions and friction with the seeds and sunflower disks, and its own kinetic energy is retained better; thereby, it shows the most obvious trajectory.

3. Results and Analysis

3.1. Simulation Test Design

According to the analysis results of the gas–solid coupling simulation, the key factors affecting the operating effect of the cleaning device are wind speed, vibration frequency, and amplitude. Based on the standard of DG/T182-2019 "Self-Propelled Sunflower Seed Harvester" [28], the orthogonal rotary combination test was conducted using EDEM software with the loss rate Y_1 and the impurity rate Y_2 of the cleaned grains serving as evaluation indices. The loss rate Y_1 and the impurity rate Y_2 can be calculated by the following equations:

$$\begin{cases} Y_1 = \frac{M_s}{M_0 - M_z + M_s} \times 100\% \\ Y_2 = \frac{M_z}{M_0} \times 100\% \end{cases} \tag{6}$$

In Equation (6), M_z is the mass of impurities contained in the seed box, g; M_s is the mass of seeds in the discharged impurities, g; M_0 is the total mass of sunflower seeds and impurities in the seed box, g.

3.2. Single-Factor Simulation Test

Based on the actual operation of commonly used clearing devices and a review of the related literature, the range of values of the operating parameters of the influencing factors were determined, as shown in Table 4. In accordance with the quality evaluation standard of harvesting operation of the sunflower harvester, the loss rate and impurity rate of the edible sunflower dislodged material in the cleaning operation are selected as the test indexes, and the main influencing factors of the cleaning device are subjected to a single-factor test.

Table 4. Scope of Single-Factor Test.

Factor	Wind Speed x_1/m·s^{-1}	Vibration Frequency x_2/Hz	Vibration Amplitude x_3/mm
Scope	28–36	6–10	36–44

3.2.1. One-Factor Test on Wind Speed

Keeping the vibration amplitude and vibration frequency unchanged, the parameter of wind speed was gradually changed, and the relationship between wind speed and loss rate and impurity rate was finally obtained, as shown in Figure 12.
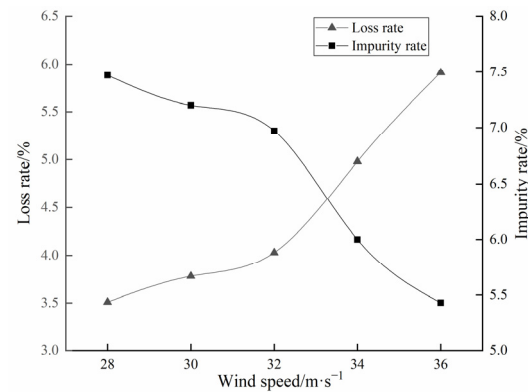
Figure 12. Effect of wind speed on loss rate and impurity rate.

When the wind speed varied within the range of 28 m·s^{-1} to 32 m·s^{-1}, the loss rate of the sunflower seeds gradually increased. Specifically, the loss rate at the end of the interval was 0.52% higher compared to that at the beginning, while the impurity rate exhibited a gradual decreasing trend within this wind speed interval, and the impurity rate at the end of the interval decreased by 0.6% compared with that at the beginning of the interval. When the wind speed was further increased and varied from 32 to 36 m·s^{-1}, the seed loss rate increased by 1.88% at a wind speed of 36 m·s^{-1} compared with that at a wind speed of 32 m·s^{-1}, and its trash content decreased by 1.54%. The results indicate that with the increase in wind speed, the cleaning device is more effective in separating smaller and lighter impurities, but at the same time it causes more loss of sunflower seeds. By comparing the changes in loss rate and impurity rate across different wind speed intervals, it can be seen that the increase in loss rate and the decrease in impurity rate in the high wind speed interval (wind speed of 32–36 m·s^{-1}) were more significant than that in the low wind speed interval (wind speed of 28–32 m·s^{-1}), and the differences of loss rate and impurity rate in the high and low wind speed intervals were 1.36% and 0.94%, respectively. Considering the variation in both loss rate and impurity rate, when the wind speed varied within the interval of 30–34 m·s^{-1}, the operational performance of the cleaning device was superior.

3.2.2. One-Factor Test on Vibration Frequency

Keeping the wind speed and vibration amplitude unchanged, we gradually changed the vibration frequency and obtained the loss rate and impurity rate with the vibration frequency of the graph, shown in Figure 13.

In the vibration frequency interval of 6–8 Hz, the loss rate decreased by 0.41%, whereas in the interval of 8–10 Hz, it increased by 1.48%; in the whole vibration frequency range of 6–10 Hz, the impurity rate decreased by 1.22% in general. As the vibration frequency increased, the loss rate of edible sunflower seeds showed a tendency of decreasing and then increasing, while the impurity rate consistently decreased. At low vibration frequencies, the movement of sunflower dislodged material on the vibrating screen was relatively smooth, preventing impurities from being thrown out. This resulted in seeds accumulating on the screen surface along with impurities, leading to higher loss rates and impurity content. However, as the vibration frequency gradually increased, the sunflower dislodged material on the screen surface began to move significantly, prompting the sunflower seeds to move easier in the vibration through the sieve hole, while the lighter impurities are also more easily thrown out, so the loss rate and the impurity rate in the vibration frequency range of

6–8 Hz show a downward trend. When the vibration frequency reaches 8 Hz, the loss rate shows an inflection point; at this time, with the increase in vibration frequency, the loss rate begins to rise rapidly. Through comprehensive analysis, it can be seen that in the vibration frequency interval of 7–9 Hz, the cleaning effect of sunflower seeds is better.
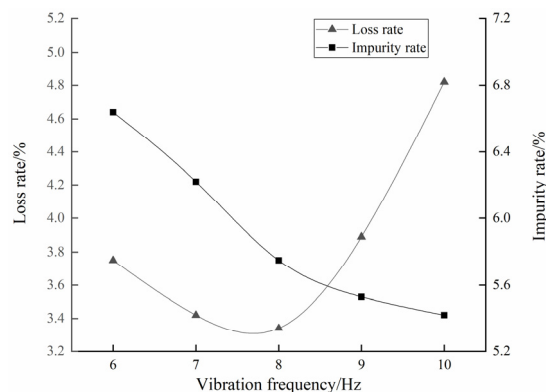
Figure 13. Effect of vibration frequency on loss rate and impurity rate.

3.2.3. One-Factor Test on Vibration Amplitude

Keeping the wind speed and vibration frequency unchanged, we gradually changed the vibration amplitude, and obtained the loss rate and impurity rate with the vibration amplitude of the graph, shown in Figure 14.
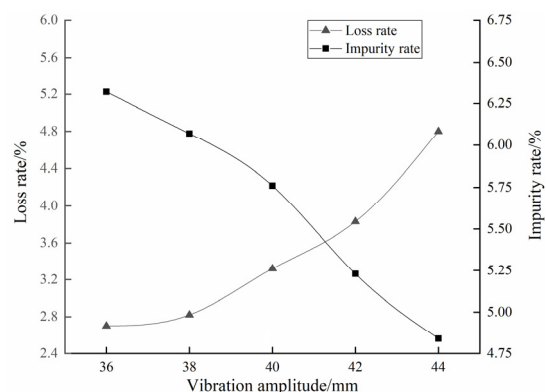
Figure 14. Effect of vibration amplitude on loss rate and impurity rate.

When the vibration amplitude is at a low level, the movement amplitude of the edible sunflower dislodged material on the surface of the vibrating screen is small, resulting in minimal displacement in both the vertical and the horizontal directions. This leads to poor layering of the material by the device, ultimately causing a high impurity rate in the cleaned seeds. As the vibration amplitude increases, the vertical and horizontal displacements of the throwing motion increase, and the lightweight impurities are thrown out smoothly, reducing the impurity rate of the edible sunflower seeds. However, the increase in amplitude diminishes the chances of contact between the seeds and the sieve surface, which hinders the passage of seeds through the sieve holes and consequently leads to an increase in seed loss. The magnitude of change in the values of loss rate and impurity rate in the high vibration amplitude range (vibration amplitude: 40–44 mm) was higher than that in the low amplitude range (vibration amplitude: 36–40 mm) by 0.86% and 0.36%, respectively, so that the change in loss rate and impurity rate was more significant in the higher amplitude range for the same increase in vibration amplitude. By comprehensively comparing the values of the two evaluation indexes, it can be seen that when the value of the vibration amplitude is in the vibration amplitude interval of 38–42 mm, the performance of the cleaning device is relatively better.

3.3. Orthogonal Simulation Test

In order to clarify the degree of influence of different factors on the threshing effect and to obtain the optimal combination of operating parameters, orthogonal tests were carried out. The test factor level values of wind speed, vibration frequency, and amplitude were selected from the results of the previous single-factor simulation test, as shown in Table 5.

Table 5. Table of Test Factor Level.

Level	Coding Factor		
	Wind Speed $x_1/m \cdot s^{-1}$	Vibration Frequency x_2/Hz	Vibration Amplitude x_3/mm
−1	30	7	38
0	32	8	40
1	34	9	42

3.4. Analysis of Orthogonal Simulation Test Results

The orthogonal test scheme is designed by Design-Expert10 (The Design-Expert10 is developed by Stat-Ease, Inc., a company located in the United States.), and the simulation parameters are adjusted in the simulation software for the scheme to carry out the test. The orthogonal test results are shown in Table 6.

Table 6. Results of the orthogonal test.

No.	Wind Speed $x_1/m \cdot s^{-1}$	Vibration Frequency x_2/Hz	Vibration Amplitude x_3/mm	Loss Rate $Y_1/\%$	Impurity Rate $Y_2/\%$
1	1	0	1	4.4	5.63
2	−1	0	−1	3.12	6.35
3	−1	1	0	3.42	6.18
4	1	0	−1	3.74	5.95
5	1	−1	0	4.08	5.89
6	−1	0	1	3.59	6.07
7	1	1	0	4.17	5.77
8	0	0	0	3.63	6.12
9	0	1	1	4.05	5.91
10	0	−1	−1	3.34	6.42
11	0	1	−1	3.68	6.2
12	0	0	0	3.53	6.18
13	−1	−1	0	3.22	6.43
14	0	0	0	3.67	6.03
15	0	0	0	3.66	6.15
16	0	−1	1	3.91	6.14
17	0	0	0	3.7	5.97

By processing the results of orthogonal tests, the following quadratic polynomial regression model can be obtained regarding the loss rate and the impurity rate of sunflower seeds:

$$Y_1 = 3.64 + 0.38x_1 + 0.0962x_2 + 0.2587x_3 - 0.0275x_1x_2 + 0.0475x_1x_3 - 0.05x_2x_3 + 0.026x_1^2 + 0.0585x_2^2 + 0.0485x_3^2 \tag{7}$$

$$Y_2 = 6.09 - 0.2237x_1 - 0.1025x_2 - 0.1463x_3 + 0.0325x_1x_2 - 0.01x_1x_3 - 0.0025x_2x_3 - 0.095x_1^2 + 0.0725x_2^2 + 0.005x_3^2 \tag{8}$$

The analysis of variance (ANOVA) table for the loss rate and the impurity rate of sunflower seeds is shown in Table 7.

Table 7. Analysis of variance for regression equations.

Source	Loss Rate				Impurity Rate			
	Sum of Squares	Degree of Freedom	F-Value	*p*-Value	Sum of Squares	Degree of Freedom	F-Value	*p*-Value
Model	1.82	9	46.86	<0.0001 ***	0.7176	9	16.90	0.0006 ***
x_1	1.16	1	268.16	<0.0001 ***	0.4005	1	84.89	<0.0001 ***
x_2	0.0741	1	17.20	0.0043 **	0.0840	1	17.82	0.0039 **
x_3	0.5356	1	124.33	<0.0001 ***	0.1711	1	36.27	0.0005 ***
x_1x_2	0.0030	1	0.7022	0.4297	0.0042	1	0.8955	0.3755
x_1x_3	0.0090	1	2.10	0.1910	0.0004	1	0.0848	0.7794
x_2x_3	0.0100	1	2.32	0.1714	0.0000	1	0.0053	0.9440
x_1^2	0.0028	1	0.6607	0.4431	0.0380	1	8.05	0.0251 *
x_2^2	0.0144	1	3.34	0.1101	0.0221	1	4.69	0.0670
x_3^2	0.0099	1	2.30	0.1732	0.0001	1	0.0223	0.8855
Residual	0.0302	7			0.0330	7		
Lack of Fit	0.0131	3	1.02	0.4719	0.0024	3	0.1057	0.9524
Pure Error	0.0171	4			0.0306	4		
Total	1.85	16			0.7506	16		

Note: * significant ($p < 0.05$); ** very significant ($p < 0.01$); *** extremely significant ($p < 0.001$).

The regression analysis table of loss rate and impurity rate reveals that the *p*-values of the Y_1 and Y_2 regression models are less than 0.001, indicating that the two corresponding regression models are highly significant. Furthermore, the *p*-value of lack of fit of the two regression models is greater than 0.01. The coefficients of determination and the correction coefficients of determination of the two models are close to 1, which indicates that the regression models of the loss rate and the impurity rate obtained from the experiment have a higher degree of reliability. In both models, the regression terms x_1 and x_3 were found to be extremely significant, while x_2 was significant, and there was no interaction between the factors.

The perturbation diagram facilitates a comparison of the effects of the three influencing factors on the evaluation indexes within a specific level range. The perturbation diagram of the influence of each factor on the rate of seed loss is shown in Figure 15, where A, B, and C represent wind speed, vibration frequency, and amplitude, respectively. Under the influence of different levels of these factors, the maximum values of loss rate were 4.04%, 3.78%, and 3.94%, respectively, and the minimum values of loss rate were 3.28%, 3.60%, and 3.42%, respectively. By analyzing the direction of the three curves in the perturbation diagram, it becomes evident that wind speed, frequency, and amplitude are positively correlated with the loss rate of sunflower seeds. Among these factors, vibration frequency (B) exhibits the smallest effect on the loss rate of sunflower seeds, with the most gentle trend in its curve. The change in wind speed (A) has the greatest impact on the loss rate, and the trend of the curve changes the most drastically. The effect of vibration frequency (B) and amplitude (C) on the loss rate at low levels is significantly lower than that on the grain loss at high levels. This phenomenon is mainly due to the fact that when the amplitude or vibration frequency is at a high level, the movement of detached grains on the surface of the vibrating screen is more intense, and the probability of the grains being thrown out of the working surface increases in the process, leading to a change in the magnitude of the grain loss rate.

The perturbation diagram illustrating the impact of each factor on the impurity rate of seeds is depicted in Figure 16. where A, B, and C represent wind speed, vibration frequency, and amplitude, respectively. At different levels of wind speed, vibration frequency, and amplitude, the maximum and minimum values of impurity rate were observed. The maximum values were 6.21%, 6.26%, and 6.24%, respectively, while the minimum values were 5.76%, 6.05%, and 5.94%. As the levels of wind speed, vibration frequency, and amplitude increased, the overall trend of the impurity rate of seeds exhibited a continuous

decrease. In terms of the magnitude of reduction in impurity rate, the effect of a change in wind speed was more significant than that brought about by the changes in amplitude and frequency of vibration. When wind speed was varied within the high wind speed interval, its effect on the impurity rate was greater than when it was varied in the lower wind speed interval. In contrast, changes in vibration frequency in the low level interval have a significantly greater effect on the impurity rate than changes in the high level interval.
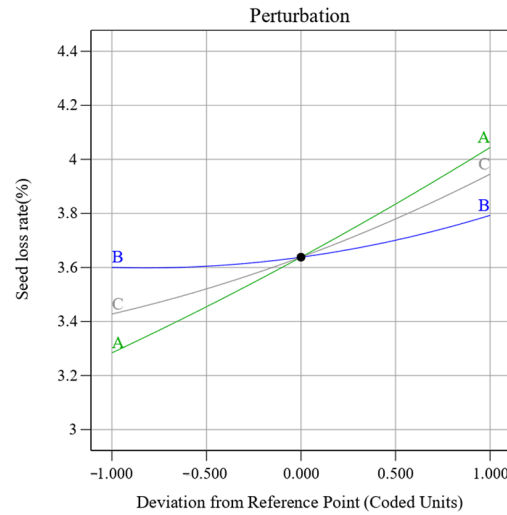
Figure 15. Perturbation plot: Effect of factors on loss rate of sunflower seeds.
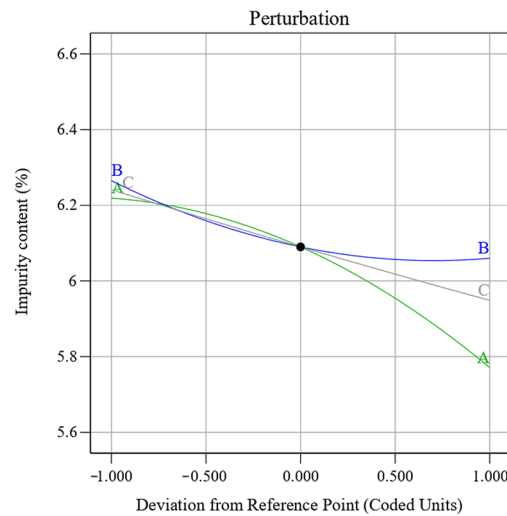
Figure 16. Perturbation plot: Effect of factors on impurity rate of sunflower seeds.

3.5. Parameter Optimization

According to the results of the orthogonal simulation test, the parameters of the test are optimized using the parameter optimization module that comes with Design-Expert. According to the boundary conditions of each parameter of the orthogonal test and the requirements of the objective function, the constraints of the objective function are set as follows:

$$\begin{cases} \min Y_1(x_1, x_2, x_3) \\ \min Y_2(x_1, x_2, x_3) \\ 30 \text{ m} \cdot \text{s}^{-1} \leq x_1 \leq 34 \text{ m} \cdot \text{s}^{-1} \\ 7 \text{ Hz} \leq x_2 \leq 9 \text{ Hz} \\ 38 \text{ mm} \leq x_3 \leq 42 \text{ mm} \end{cases} \tag{9}$$

Based on the above constraints, the objective function is solved using the parameter optimization module of Design-Expert. The final result is as follows: the optimal air speed is 30 m/s, the optimal vibration frequency is 8.44 Hz, and the optimal amplitude is 41.35 mm.

3.6. Bench Validation Test

In order to ascertain the reliability of the optimal parameters obtained from the orthogonal simulation test, a test bench for the cleaning device was constructed and the results of the bench test were compared and analyzed with those of the simulation test.

3.6.1. Test Materials and Equipment

The material used in the validation test was Sanrui No. 39 sunflower planted in Urumqi County, Xinjiang.

Instruments required for the validation test: homemade sunflower cleaning device bench (Figure 17), tachometer (range 10–99,999 rpm, accuracy 0.01 rpm, measurement error ± (0.04% + 2d)), electronic scales (range 1–50,000, accuracy 0.1 g), AE200H frequency converter inverter (rated power of 3 kW, rated voltage of 380 V, speed ratio 1:100).

Figure 17. Sunflower cleaning device.

3.6.2. Test Method

Before the test, 20 kg of the edible sunflower dislodged materials were precisely weighed using an electronic weighing scale and uniformly arranged in the feed box within 4 s. With the vibration of the vibrating sieve, the edible sunflower dislodged materials were continuously dropped into the screen mesh, and when all the objects were cleaned, the mass of the seeds, the mass of the impurities, and the seeds contained in the impurities were weighed, and we calculated the loss rate and impurity rate according to the formula. To ensure the effectiveness of the cleaning device, the working parameters for the bench test were chosen based on the optimal parameters derived from the orthogonal simulation test. To minimize errors in the test data, the bench test was repeated five times. After that, the simulation test was also conducted in EDEM2018. The parameter settings in the simulation test were the same as those in the actual bench test, and the test was also carried out five times. Finally, the results of the simulation test and the bench test were compared and analyzed to determine whether the actual clearing effect of the device is consistent with the results simulated by the software.

3.6.3. Analysis of the Results of Bench Validation Test

The data comparison graph between the results of the bench validation test and the simulation test is shown in Figure 18. The average loss rate of sunflower seeds from the bench test was 3.59% and the average impurity rate was 6.36%, while the average loss rate

of sunflower seeds from the simulation test was 3.47% and the average impurity rate was 6.17%, and the relative errors of loss rate of sunflower seeds and impurity rate were 3.45% and 3.07%, respectively, which were both less than 5% between the two tests. Therefore, the results of the simulation test are reliable.
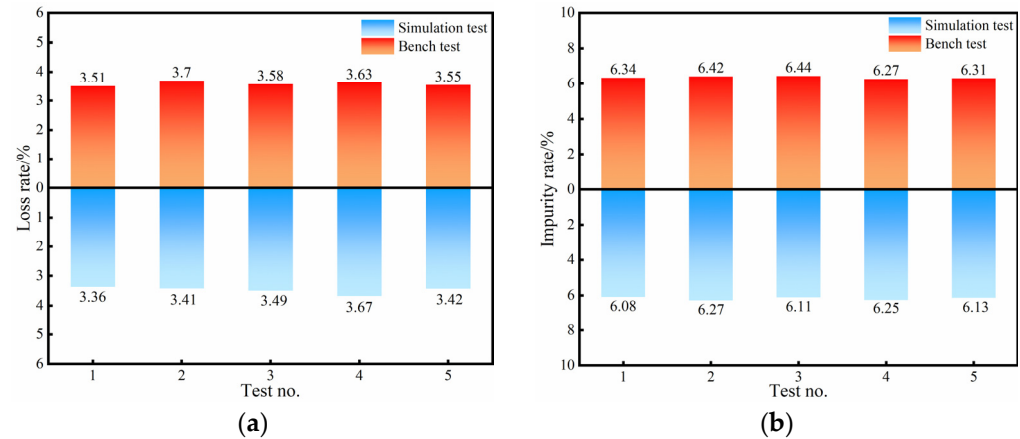
Figure 18. Comparison of the results of the bench validation test and the simulation test. (**a**) Comparative graph of seed loss rate. (**b**) Comparative graph of seed impurity rate.

Through the comparative analysis of the bench test and the simulation test, it was found that the seed loss rate and the impurity rate obtained from the bench test were significantly higher than the results of the simulation test. The main reasons for this phenomenon include the following:

1. The simulation model is too ideal. The simulation model ignored the existence of light impurities. For example, in the bench test, during the process of the sunflower disks shaking, the dried leaves attached to the edge of the disk may fall off to some extent, while in the simulation, the broken sunflower head is treated as a whole, thereby ignoring the shedding of leaves on the disk.

2. The simulation failed to fully consider the effect of moisture contained in the discharged material on the cleaning effect, while in the actual bench test, the moisture contained in the discharged material would cause adhesion between the impurities and the seeds, which would make it more difficult for the light impurities to be removed by the cleaning device, thus affecting the final cleaning effect.

3. When the sieved grains are picked out from all the impurities and weighed, the surface of the grains will inevitably be coated with dust and impurities due to electrostatic adsorption, which leads to a larger calculated loss rate of the grains.

4. In the bench test of sunflower, the threshed materials are manually introduced into the feed box, while in the simulation, particles are synthetically generated by the granule factory according to a normal distribution. This relative error in feeding of the threshed materials may lead to higher loss rate and impurity content of sunflower seeds in the bench test.

4. Discussion

Sunflower is widely planted in China due to its short growth period, strong adaptability, and low planting cost. However, the current level of sunflower machinery harvest in China is generally low, which significantly limits the development and promotion of sunflower in the country. As an essential process in the mechanical harvesting of sunflower, the cleaning performance directly determines the final harvest quality of sunflower seeds. Therefore, it is crucial to study and explore the cleaning device of sunflower harvesters. In this paper, we started by considering the material characteristics of edible sunflower discharged material. We simulated the scavenging operation process of the device by FLUENT-DEM gas–solid coupling technology, analyzed the velocity, velocity vector, and

discharged material motion law in the cleaning device, explored the operation factors that have important influence on the performance of the cleaning, and derived the optimal combination of operation parameters by using the orthogonal test, and then carried out the bench test of the cleaning device under the optimal parameter combination, so as to validate the accuracy of the simulation process and the conclusions. Under the optimal parameter combination, the seed loss rate and impurity rate can reach 3.47% and 6.17%, respectively, meeting the criteria that the loss rate of sunflower kernel cleaning is less than 3.5% and the impurity rate is less than 18%. Compared with the existing cleaning device, the cleaning ability of this device has been improved to a large extent: the device has a simple structure and is more targeted to edible sunflower, and the ability to deal with the edible sunflower dislodged material is stronger, has higher efficiency, and is more adaptable to the working intensity of the sunflower harvester.

Reflecting on our work in this paper, while some research results have been achieved, there are some shortcomings for improvement. Firstly, in this study, the motion mode of the vibrating sieve is a simple repetitive round-trip motion. The motion mode is single, and the effect of not passing the form of motion on the cleaning work of the vibrating screen is not considered. The CFD-DEM-MBD coupling technology can be utilized in future related research to explore the cleaning performance of vibrating sieves with different motion modes. Secondly, this study is limited to the design of a single-material rigid sieve, without considering of material suitability or the cleaning process. The possibility of rupture and loss of edible sunflower seeds is greater, which means that the cleaning device cannot then perform at its optimal level in its normal mode of movement. Further research on elastic sieves could be conducted to analyze the impact of the vibrating screen with different materials on the performance of the cleaning process. Lastly, due to the seasonal nature of harvesting sunflowers and the structure of the device, the device is subject to more interference when the entire machine is tested in the field. Consequently, it is challenging to ascertain whether the impurity and loss rates of the collected materials are affected by nondesign factors. The collected and cleared materials are affected by other nondesign factors, which is why this study only conducted a bench test. In future research, the structure of the device can be improved, and the related inspection equipment can be added to conduct field trials in subsequent studies.

5. Conclusions

The innovation of this paper is the design of a wind-screen type cleaning device suitable for sunflower harvester in view of the existing sunflower cleaning device lacking pertinence and having low cleaning efficiency, high cleaning loss rate, and impurity rate. We designed the vibrating screen with key parameters. The vibrating screen is divided into two parts: the upper screen and the lower screen. The upper screen adopts a woven screen design with large openings to facilitate the filtration of large particles, while the lower screen adopts an innovative "round hole screen + long hole screen" combination design, which is capable of effectively separating different sizes and shapes of discharged materials. The upper sieve measures 1991 mm in length and 900 mm in width, the combined lower sieve is 1784 mm long and 900 mm wide, the tail sieve is 458 mm and 900 mm wide, with an installation angle of 8 degrees, and the relative distance between the upper and lower sieves is set at 104 mm. Subsequently, we targeted the material characteristics of edible sunflower and designed the cleaning device accordingly. We simulated the working environment of the device and the material processing using FLUENT-DEM gas–solid coupling technology. The interaction between particles and fluids was accurately simulated by coupling technology. The change rule of wind speed, the distribution of airflow in the device, and the intensity change were clarified, and the key factors affecting the working effect of the scavenging device as well as the three kinds of the edible sunflower dislodged materials were obtained in the movement condition in the actual work. Finally, an orthogonal simulation test was conducted for the key parameters influencing the working effectiveness of the scavenging device, as derived from the coupling analysis. This test

allowed for a preliminary evaluation of the scavenging device's performance and we obtained the identification of an optimal combination of working parameters. The test bench for the cleaning device was also manufactured. The bench test and simulation test were carried out based on the optimal parameter combinations obtained. The simulation test results and bench test results under the same parameters were compared and analyzed, which verified the reasonableness of the design of the device and the reliability of the simulation analysis. This device has improved the current situation in Xinjiang where there is a lack of cleaning devices specifically designed for the characteristics of edible sunflower seeds, enhancing the cleaning efficiency of the edible sunflower. This provides a reference for the design and improvement of future sunflower cleaning devices.

References

1. Liu, H.M. Development trend of edible sunflower. *Mod. Agric.* **2018**, *2*, 56.
2. Statistics of Sunflower Seed Industry Data in 2023: The Sunflower Seed Planting Area in China Reached 26 Million Tons. [EB/OL]. Available online: https://www.chinabgao.com/k/kuihuazi/68605.html (accessed on 5 April 2024).
3. Chen, Z. Analysis and Prediction of National Edible Sunflower Cultivation in 2019 [EB/OL]. Available online: http://www.360doc.com/content/19/0529/22/29650793_839079859.shtml (accessed on 7 April 2024).
4. Zong, W.Y.; Liu, Y.; Huang, X.M.; Ma, L.N.; Tang, S.P. Research status and development countermeasures of mechanized harvesting of sunflower. *J. Jiangxi Agric. Univ.* **2017**, *39*, 600–606.
5. Chen, L. Design and Experimental Research on the Cleaning Device of Rapeseed Combine Harvester. Master's Thesis, Huazhong Agricultural University, Wuhan, China, 2013.
6. Du, Y.F.; Mao, E.R.; Zhu, Z.X.; Wamg, X.J.; Yue, X.W.; Li, X.Y. Design and test of cutting table of two rows corn harvester. *J. Agric. Mach.* **2013**, *44* (Suppl. S2), 21–22.
7. Chen, Z.; Hao, F.P.; Wang, F.D.; Su, W.F.; Cui, J.W. Research on the development of corn harvesting technology and equipment in China. *J. Agric. Mach.* **2012**, *43*, 47–49.
8. Zou, L.; Zhuo, J.Q.; Yang, R.Q. Analysis of the development prospect of corn harvester in China. *Res. Agric. Mech.* **2008**, *4*, 205–208.
9. Liu, Y. Overall Design of Sunflower Harvester and Experimental Research on Picking Device. Master's Thesis, Xinjiang Agricultural University, Urumqi, China, 2017.
10. Bulgakov, V.; Kiurchev, S.; Ivanovs, S.; Olt, J. Experimental substantiation of parameters of aspiration separator of sunflower seeds. *Eng. Rural.* **2020**, *19*, 435–444.
11. Ueka, Y.; Matsui, M.; Inoue, E.; Mori, K.; Okayasu, T.; Mitsuoka, M. Turbulent Flow Characteristics of the Cleaning Wind in Combine Harvester. *Eng. Agric. Environ. Food* **2012**, *5*, 102–106. [CrossRef]
12. Priporov, I.E.; Kurasov, V.S.; Samurganov, E.E.; Shepelev, A.B. Modeling the sunflower seeds separation process in air-sieve grain-cleaning machines. *IOP Conf. Ser. Mater. Sci. Eng.* **2021**, *1111*, 012048. [CrossRef]
13. Priporov, I.E. Mathematical model of the separation process of sunflower seeds in innovative air-sieve grain-cleaning machine. *Bulg. J. Agric. Sci.* **2022**, *28*, 362–366.
14. Craessaerts, G.; Saeys, W.; Missotten, B.; De Baerdemaeker, J. A genetic input selection methodology for identification of the cleaning process on a combine harvester, Part I: Selection of relevant input variables for identification of the sieve losses. *Biosyst. Eng.* **2007**, *98*, 166–175. [CrossRef]
15. Craessaerts, G.; Saeys, W.; Missotten, B.; De Baerdemaeker, J. Identification of the cleaning process on combine harvesters. Part I: A fuzzy model for prediction of the material other than grain (MOG)content in the grain bin. *Biosyst. Eng.* **2008**, *101*, 42–49. [CrossRef]

16. Craessaerts, G.; Saeys, W.; Missotten, B.; De Baerdemaeker, J. A genetic input selection methodology for identification of the cleaning process on a combine harvester, Part II: Selection of relevant input variables for identification of material other than grain (MOG)content in the grain bin. *Biosyst. Eng.* **2007**, *98*, 197–303. [CrossRef]
17. Grozubinsky, V.; Sultanovitch, E.; Lin, I.J. Efficiency of solid particle screening as a function of screen slot size, particle size, and duration of screening. *Int. J. Miner. Process.* **1998**, *52*, 261–272. [CrossRef]
18. Fattahi, S.H.; Abdollahpour, S.; Ghassemzadeh, H.; Behfar, H.; Mohammadi, S.A. Regression model of sunflower seed separation and theinvestigation of its germination in corona field. *Agric. Eng. Int.* **2017**, *19*, 187–192.
19. Zhang, J.X.; Wang, Y.C.; Cai, Y. Upright Centrifugal Oil Sunflower Threshing and Cleaning Device. CN110800472B, 27 May 2022.
20. Pan, Z.Y. *Numerical Simulation and Test of Forced Inertia Separation Chamber*; Northeast Agricultural University: Harbin, China, 2014.
21. Liu, K.; Jiang, E.C.; Wang, L.J. Numerical simulation of gas-solid two-phase flow in the inertial separation chamber of a combine harvester. *J. Jiangsu Univ. Nat. Sci. Ed.* **2006**, *27*, 193–196.
22. Hou, J.M.; Ren, Z.T.; Zhu, H.J. Design and test of double-deck inclined vibrating wind screen type castor clearing device. *J. Agric. Mach.* **2022**, *53* (Suppl. S2), 39–51.
23. Mechanical Research Institute of the First Ministry of Machinery. In *Agricultural Machinery Design Manual*; Machinery Industry Press: Beijing, China, 1973.
24. Li, B.; Li, W.N.; Bai, X.B. Study on sieving rate of tea fresh leaf classifier based on EDEM. *Tea Sci.* **2019**, *4*, 484–494.
25. Li, Y. Research on the Motion Law of Gas-Solid Two Phases in Corn Wind Sieve Cleaning Device. Master's Thesis, Northeast Agricultural University, Harbin, China, 2015.
26. Sun, X.; Li, B.; Liu, Y.; Gao, X. Parameter Measurement of Edible Sunflower Exudates and Calibration of Discrete Element Simulation Parameters. *Processes* **2022**, *10*, 181. [CrossRef]
27. Li, H.; Wang, J.; Yuan, J.; Yin, W.; Wang, Z.; Qian, Y. Analysis of threshed rice mixture separation through vibration screen using discrete element method. *Int. J. Agric. Biol. Eng.* **2017**, *10*, 231–238.
28. *DG/T182-2019*; Self-Propelled Sunflower Seed Harvester. Ministry of Agriculture and Rural Affairs of the People's Republic of China: Beijing, China, 2019.